SELF-FORMATION OF Fe/Fe-O NANOPARTICLES IN POROUS SiO$_2$ FILMS *

I. Šimkienė [a,b], J. Sabataitytė [a,c], M. Baran [d], R. Szymczak [d], J.-G. Babonas [a,c], A. Rėza [a,e], and A. Kaliničenko [f]

[a] *Semiconductor Physics Institute, A. Goštauto 11, LT-01108 Vilnius, Lithuania*
[b] *Vilnius University, Saulėtekio 9, LT-10222 Vilnius, Lithuania*
[c] *Vilnius Gediminas Technical University, Saulėtekio 11, LT-10223 Vilnius, Lithuania*
[d] *Institute of Physics, PAN, Al. Lotnikow 32/46, 02-668 Warsaw, Poland*
[e] *Vilnius Pedagogical University, Studentų 39, LT-08106 Vilnius, Lithuania*
[f] *Institute of Chemistry, A. Goštauto 10, LT-01108 Vilnius, Lithuania*

Self-formation of Fe/Fe-O particles in porous SiO$_2$ films has been studied by investigating the structure and physical properties of hybrid samples SiO$_2$:Fe/SiO$_2$/Si. The sol–gel spin-on technique was used for the formation of Fe-doped silica films on silica-coated Si wafers. The sol was prepared from precursors composed of ethanol and/or aqueous solutions of tetraethoxysilane (TEOS) and FeCl$_3$. As-grown hybrid samples were annealed in Ar atmosphere. Structural studies by means of atomic force microscopy (AFM) have shown a different morphology of samples produced from precursors with various Fe-amount. Spectroscopic ellipsometry measurements were carried out for characterization of the contribution of Fe/Fe-O clusters to the optical response of hybrid samples. Magnetic properties of Fe-doped silica films were studied by measuring the magnetic field and temperature dependences of magnetization. Experimental data were interpreted taking into account particular features of Fe and Fe-O nanoparticles in silica matrix.

Keywords: nanoscale materials and structures, fabrication and characterization

PACS: 81.07.-b, 81.16.Dn

1. Introduction

Self-formation is a general principle describing the structural ordering of the system without external influence [1]. During the last decade, this principle was used in nanotechnology as the "bottom-up" technique to arrange structurally the assembly of nanometric particles [2]. For example, the self-assembled system of colloidal nanoparticles can form, on the one hand, the diamond-like structure with the properties typical of photonic crystal [3]. On the other hand, porous matrices of metals, metal oxides, and semiconductors can be grown from colloidal solution under specific technological conditions [4].

Recently, low-cost room-temperature sol–gel process was applied in nanotechnology [5], in particular in the formation of porous insulating matrices [6]. The sol–gel technique provides also a convenient method to obtain hybrid samples using precursors presenting the mixture of various materials. The self-formation of magnetic nanoparticles in nanopores of insulating matrices was widely studied in bulk samples [6]. However, instead of bulk insulating matrices, multilayer structures produced by planar technology using a spin-on technique are the most promising systems for practical applications. Silica layers of controlled porosity were produced on Si wafers by varying the technological procedure [7]. It was found that physical properties of hybrid samples containing Fe/Fe-O particles in silica on Si depended critically on the chemical composition of precursors (FeCl$_3$ and Fe(CH$_3$COO)$_3$) [8], technological procedure ("one-pot" and "two-pots" technique) [9], as well as on the post-growth thermal treatment in various atmospheres (air, Ar, and H$_2$) [7]. The magnetic properties were mostly expressed in the SiO$_2$:Fe/SiO$_2$/Si samples annealed in hydrogen [8].

In this work, hybrid samples SiO$_2$:Fe/Si, which have been produced from FeCl$_3$ precursor and annealed in Ar atmosphere, were studied. The structure of self-organized Fe/Fe-O clusters in silica was investigated by

atomic force microscopy (AFM). The optical response and magnetization of hybrid samples were analyzed and correlated with particular features of the structure.

2. Experimental

The hybrid samples SiO_2:Fe/Si were prepared by sol–gel spin-on technique described in [8] in more detail. The aqueous solution of $FeCl_3$ was mixed with either freshly prepared colloidal ethanol solution of tetraethoxysilane (TEOS) ("one-pot" reaction) or with structurized TEOS sol ("two-pots" reaction). The acidity of coating solutions was in the range of pH values 1.9–2.1. The coating solution was deposited by spinning at 2500 rpm on n-Si (0.5 Ω·cm) (100)-oriented wafers, which usually have been already coated by silica using the same sol–gel spin-on technique. Multiple layer structures composed of one or two Fe-doped silica layers on up to four silica layers were prepared. After deposition of each layer, the samples were dried in air at 95 °C for 0.5 h and the hybrid samples SiO_2:Fe/SiO_2/Si were annealed in Ar atmosphere at 550 °C for 2 h and then cooled down in the same atmosphere to room temperature.

The structure of the samples was investigated by a standard atomic force microscope (AFM) Thermomicroscope Explorer. The optical properties of the samples were studied by means of spectroscopic ellipsometer with rotating analyzer operating at room temperature in the range of 1–5 eV. The spectra of ellipsometric parameters Ψ and Δ were analyzed in a multilayer model [8]. The magnetization of the samples was measured as a function of magnetic field (up to 5 T) and temperature (5–300 K) using a commercial SQUID magnetometer (MPMS-5, Quantum Design). The magnetic field was oriented in the plane of the films.

3. Results and discussion

3.1. Structural features

The process of self-formation of Fe-containing nanoparticles and clusters depends on chemical composition of precursor, conditions of growth procedure, and post-growth thermal treatment [7–9]. The hybrid samples under investigation were prepared from the same precursor containing $FeCl_3$ and annealed in the same Ar atmosphere. Thus, the intrinsic structure of Fe-doped films depended mainly on the growth conditions.

As noted above, the Fe-doped silica layer was usually deposited on the silica-coated Si wafers. The sol–
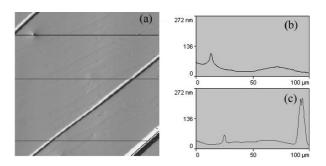

Fig. 1. (a) Morphology and surface roughness profile at (b) upper and (c) lower horizontal lines shown in (a) of thick ($d \sim 800$ nm) Au-decorated SiO_2 layer. The surface area in (a) AFM micrograph is 100×100 μm^2.

gel spin-on processed silica layers on the Si surface, which have been dried at ~ 100 °C for 1 h, were dense with porosity of $\sim 10\%$ at the centre of Si wafer with diameter of 5 cm, and 5% at the edge [10]. However, when Si wafers of a smaller diameter (1–2 cm) were used, the roughness of the surface was ~ 250 nm due to formation of clusters composed of rectangular-shaped particles of size $\sim 50 \times 50$ nm^2 and ~ 50 nm in height [10]. The cracks were revealed on Au-decorated thick silica films (Fig. 1) of thickness $d \geq 800$ nm. It is interesting to note that the cracks, which were most probably due to large internal stress in silica layer, were oriented along crystallographic axes of Si (100) wafers.

When aqueous solution of the salt $FeCl_3 \cdot 6\,H_2O$ is prepared, the hydrolysis takes place:

$$FeCl_3 + 3H_2O = Fe(OH)_3\downarrow + 3HCl. \qquad (1)$$

As the solution is prepared at room temperature, the hydrolysis is not an intensive process. As a result, on the one hand, $FeCl_3$ was not completely hydrolized. On the other hand, active molecules of $Fe(OH)_3$ joined together as $Fe(OH)_m$ forming the core of colloidal particle, at the surface of which Fe^{3+} ions were adsorbed. In the precursor solution, the $Fe(OH)_m$ particles form the complexes with the particles of silicon hydroxide due to intensive hydrolysis and condensation of TEOS. As a result of these chemical reactions, significant amount of excess water is present in the Fe-doped layer deposited on Si wafer in the sol–gel spin-on process.

Annealing in Ar atmosphere at a relatively high temperature (550 °C), in contrast to thermal treatment in H_2 [8], leads to an intensive water evaporation and local destruction of Fe-doped SiO_2 film (Fig. 2). The defects of size $l \sim 30$ μm and height $h = 1.3 - 1.5$ μm were seen on the surface of these hybrid samples. It should be noticed (Fig. 2) that the defect of this type presented the centre where Fe particles were accumulated from surroundings of ~ 50 μm size. Micro-
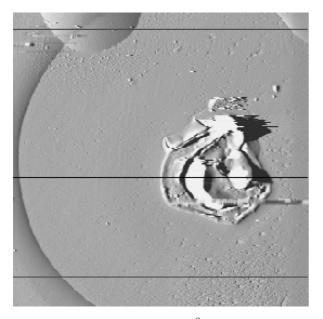
Fig. 2. AFM micrograph (100×100 μm^2) of Fe-doped film in the vicinity of defect formed due to intensive water evaporation.

analysis of chemical composition confirmed [8] the formation of Fe-depleted region around the defects. This observation indicates that accumulation of Fe-containing clusters is closely related to the hydroxides of Fe and Si. Indeed, as is known [11], iron oxides and hydroxides adsorb intensively the water molecules. As a result, Fe(OH)$_m$ clusters are surrounded by water molecules. When Fe-doped films were dried at $\sim$100 °C, iron hydroxide transformed to goethite (α-FeOOH) or lapidocrocite (γ-FeOOH):

$$\mathrm{Fe(OH)_3} = (\alpha, \gamma)\text{-FeOOH} + \mathrm{H_2O} \,. \qquad (2)$$

Analysis of chemical reactions [12] allows one to assume that in Ar-annealed Fe-doped films, i.e., at annealing in oxygen-depleted atmosphere, Fe-oxides formed nanoparticles of magnetite Fe$_3$O$_4$ and maghemite γ-Fe$_2$O$_3$, in contrast to H$_2$-annealed Fe-doped silica, in which mainly metal Fe nanoparticles were formed [8]. Under oxidation, magnetite Fe$_3$O$_4$ transformed to γ-Fe$_2$O$_3$.

As follows from Fig. 3, the self-formation of Fe clusters in Fe-doped SiO$_2$ layers is a complicated process resulting in occurrence of large meso ($l \sim 20$ μm, $h \sim 1.5$ μm), macro ($l \sim 5$ μm, $h \sim 0.5$ μm), and micro ($l \sim 1$ μm, $h \sim 150$ nm) clusters. However, as seen from Fig. 3(b), the clusters composed of isolated nanoparticles ($l \sim 50 - 100$ nm, $h \sim 20 - 50$ nm) were inserted into the pores of silica background forming rectangular plates ($l \sim 500$ nm, $h \sim 10 - 20$ nm).

Figure 4 illustrates a different shape of Fe-containing particles in hybrid SiO$_2$:Fe/SiO$_2$/Si samples, in which SiO$_2$ structure of rectangular-shaped plates was not clearly developed. On the one hand (Fig. 4(a)), large ring-like structures ($\sim$10 μm) and macro clusters composed of nanoparticles ($l = 50 - 200$ nm, $h = 10 - 20$ nm) were formed. On the other hand (Fig. 4(b)), Fe-depleted regions ($\sim 10 - 20$ μm), from which Fe-containing nanoparticles accumulated into macroclusters, were also seen. This observation possibly indicates two subsequent stages of self-formation of Fe-containing clusters in SiO$_2$ layers. In the first stage (Fig. 4(a)), the Fe-nanoparticles are grouped. In the second stage (Fig. 4(b)), Fe-containing particles from neighbouring area accumulate into macrocluster. The difference in the shape of macroclusters in various samples (compare Figs. 2 and 4(b)) can be caused by different content of water, which has evaporated at the drying and annealing processes.

3.2. Optical properties

As it is known [13], ellipsometry is a very sensitive technique for detection of thin surface layers. Null-ellipsometry can be efficiently used [10] for estimation
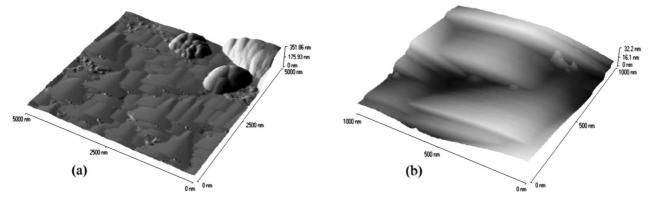

Fig. 3. (a) Small and (b) nano Fe-containing clusters on the background of silica with rectangular-like structure. The area of AFM micrograph of Fe-doped silica film in hybrid sample is (a) 5×5 μm^2 and (b) 1×1 μm^2.
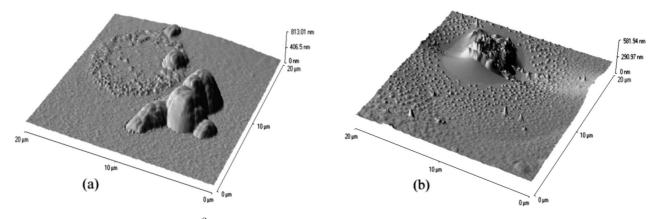
Fig. 4. AFM micrographs (20×20 μm^2) of SiO_2:Fe/SiO_2/Si hybrid samples (a) No. 33 and (b) No. 48 with higher magnetization.
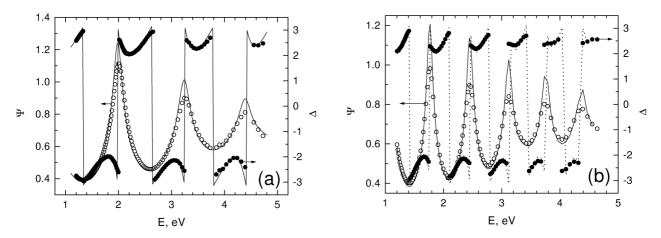

Fig. 5. Experimental (points) and modelled (curves) spectra of ellipsometric parameters characterizing the optical response of (a) two layers ($d = 390$ nm) and (b) four layers ($d = 750$ nm) of SiO_2 deposited on Si wafers.

of porosity of SiO_2 films on Si. In the case of non-homogeneous surface films, spectroscopic ellipsometry allows one to determine in-depth variation of optical characteristics [14]. When composite/hybrid films are studied, lateral non-homogeneity can be taken into account [7–9] by introducing effective medium models [15].

Figure 5 presents ellipsometric data for multiple SiO_2 layers deposited on Si by sol–gel spin-on technique. As it is seen, the interference pattern dominates in the spectra and the experimental results can be well described by the model of one effective layer with reference data for SiO_2 [16] even in the case of four SiO_2 layers deposited subsequently on Si-substrate. However, in the latter case, the average value of porosity of thick (thickness $d = 750$ nm) silica films estimated from fitting procedure increased up to 2.5% due to both intrinsic porosity and roughness. Comparison of data shown in Fig. 5 indicates that surface roughness is significant and it increases for thicker film, leading to a decrease of interferometer quality, which has not be taken into account in the present modelling.
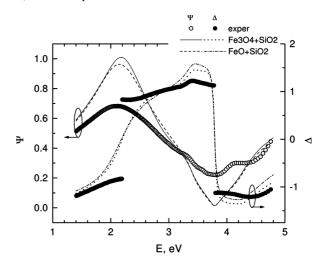

Fig. 6. Experimental (points) and modelled (curves) spectra of ellipsometric parameters in the optical response of SiO_2:Fe/Si hybrid sample with SiO_2:Fe layer grown by "two-pots" technique. The modelled spectra were calculated assuming the presence of Fe_3O_4 and FeO in SiO_2 film.

Ellipsometric data for SiO_2:Fe/Si hybrid sample produced by "two-pots" technique are shown in Fig. 6. In the calculations, reference data for magnetite Fe_3O_4
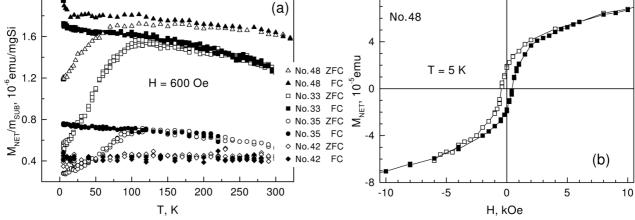
Fig. 7. (a) Temperature and (b) magnetic field dependences of magnetization in hybrid samples SiO_2:Fe/SiO_2/Si annealed in Ar atmosphere.

[17] and wustite FeO [18] were used to model the effective media composed of a mixture of iron oxides and SiO_2. As it is seen, the spectra of ellipsometric parameters are caused by a dominant contribution of interference in the SiO_2:Fe film of thickness $d \sim 120$ nm. In addition, small influence of the reflectance from SiO_2:Fe-Si interface can be noticed, which manifests itself by optical features at 3.4 and 4.3 eV characteristic of Si. However, in this case the amount of Fe-O was too small to determine particular iron oxide with a dominant contribution to the optical response.

It should be noticed that there are size limits for metal inclusions for the validity of effective media theory [19]. For example, in the case of Co in Al_2O_3, the limiting radius of metal inclusions is ∼40 nm at filling factor 0.3 for the measurements of 5% accuracy at 1 μm. In addition, corrections due to depolarization of light should be taken into account in the analysis of spectroscopic ellipsometry data [20]. Therefore, the ellipsometric data can be rather qualitatively interpreted [10, 21] by comparing the dielectric function of effective medium, which has been obtained from fitting procedure, with the reference data.

3.3. Magnetization

Figure 7 illustrates the temperature and magnetic field dependences of magnetization M in hybrid SiO_2:Fe/SiO_2/Si samples. The magnetization of hybrid samples M_{NET} was corrected by extracting magnetization of SiO_2/Si-substrates. The M_{NET}/m_{SUB} values were also normalized to the mass of each substrate. Assuming that the thickness of SiO_2:Fe films is equal in all hybrid samples, the value of M_{NET}/m_{SUB} corresponds to the magnetization of unit volume (emu/cm^3). As follows from Fig. 7(a), the

magnetization of hybrid samples with expressed structure of silica (sample No. 42) is considerably smaller than that of the samples with Fe-accumulated clusters (Nos. 33, 35, 48). The second group samples have shown similar temperature dependence of magnetization, whereas the difference in $M(T)$ values can be due to various thickness of SiO_2:Fe films. However, the variation in the temperature values, at which the difference of magnetization for the field cooled (FC) and zero-field cooled (ZFC) runs vanishes, correlates with the absolute value of magnetization M and can happen due to different mean size of Fe-containing clusters. The $M(T)$ dependences at FC runs are only slightly dependent on T, indicating that short-range magnetic interactions become significant at relatively high temperatures.

The field dependences for hybrid samples of the second group have shown the hysteresis loops (Fig. 7(b)) with the H_c values equal to 450 (5 K), 650 (25 K), and 1000 Oe (25 K) for samples Nos. 48, 33, and 35, respectively. This sequence also correlates with that for absolute M values. It should be noted that hysteresis loop for sample No. 48 is similar to that for bulk Fe-doped silica samples annealed in Ar [7].

4. Conclusion

It is concluded that in Ar-annealed hybrid SiO_2:Fe/SiO_2/Si samples, aggregates of various sizes, from nanoparticles to macroclusters, were formed. Two main types of Fe-doped films were detected. In the hybrid samples of the first type, the structure of SiO_2 layer composed of rectangular-shaped plates was developed and Fe-nanoparticles were observed. Magnetic properties of these samples were not expressed. In the hybrid samples of the second type, Fe-enriched

defects and Fe-depleted regions were observed. These samples possessed relatively strong magnetization and hysteresis loop.

Acknowledgement

References

[1] http://en.wikipedia.org/wiki/.

[2] S.C. Glotzer, M.J. Solomon, and N.A. Kotov, Self-assembly: From nanoscale to microscale colloids, Amer. Inst. Chem. Engn. **50**, 2978–2984 (2004).

[3] M. Maldovan and E.L. Thomas, Diamond-structured photonic crystals, Nature Materials **3**, 593–600 (2004).

[4] Y. Wang, Z.Y. Tang, X.R. Liang, L.M. Liz-Marzen, and N.A. Kotov, SiO_2-coated CdTe nanowires: Bristled nano centipedes, Nano Letters **4**, 225–231 (2004).

[5] P. Moriarty, Nanostructured materials, Rep. Progr. Phys. **64**, 297–381 (2001).

[6] B.J. Clapsaddle, A.E. Gash, J.H. Satcher, and R.L. Simpson, Silicon oxide in iron (III) oxide matrix: The sol–gel synthesis and characterization of Fe–Si mixed oxide nanocomposites that contain iron oxide as the major phase, J. Non-Crystal. Solids **331**, 190–201 (2003).

[7] I. Šimkienė, M. Baran, G.-J. Babonas, R.-A. Bendorius, A. Rėza, R. Szymczak, P. Aleshkevych, R. Šustavičiūtė, and R. Tamaševičius, Formation of iron-containing clusters in silica of predetermined porosity, Acta Phys. Polonica A **107**, 400–407 (2005).

[8] I. Šimkienė, J. Sabataitytė, J.-G. Babonas, A. Rėza, R. Szymczak, H. Szymczak, M. Baran, M. Kozlowski, and S. Gierlotka, Sol–gel processed iron-containing silica films on Si, Proc. SPIE 5946 (2005) (in print).

[9] G.J. Babonas, A. Reza, I. Simkiene, J. Sabataityte, M. Baran, R. Szymczak, U.O. Karlsson, and A. Suchodolskis, Optical properties of Fe-doped silica films on Si, Appl. Surf. Sci. (submitted).

[10] R. Šustavičiūtė, I. Šimkienė, J. Sabataitytė, A. Rėza, A. Kindurys, R. Tamaševičius, and J. Babonas, Formation and investigation of porous SiO_2 films on Si, Lithuanian J. Phys. **44**, 465–476 (2004).

[11] F. Jones, A.L. Rohl, J.B. Farrow, and W. Van Bronswijk, Molecular modeling of water adsorption on hematite, Phys. Chem. Chem. Phys. **2**, 3209–3216 (2000).

[12] M.P. Sharrock, Particulate magnetic recording media: A review, IEEE Trans. Magn. **25**, 4374–4389 (1989).

[13] R.M.A. Azzam and N.M. Bashara, *Ellipsometry and Polarized Light* (North-Holland, New York, 1977).

[14] J. Rivory, Characterization of inhomogeneous dielectric films by spectroscopic ellipsometry, Thin Solid Films **313–314**, 333–340 (1998).

[15] G.A. Niklasson, C.G. Granqvist, and O. Hunderi, Effective medium models for the optical properties of inhomogeneous materials, Appl. Opt. **20**, 26–30 (1981).

[16] C.M. Herzinger, B. Johns, W.A. McGaham, J.A. Woolam, and W. Paulson, Ellipsometric determination of optical constants for silicon and thermally grown silicon dioxide via multi-sample, multi-wavelength, multi-angle investigation, J. Appl. Phys. **83**, 3323–3336 (1998).

[17] W.F.J. Fontijn, P.J. van der Zaag, M.A.C. Devillers, V.A.M. Brabers, and R. Metselaar, Optical and magneto-optical polar Kerr spectra of Fe_3O_4 and Mg^{2+}- or Al^{3+}-substituted Fe_3O_4, Phys. Rev. B **56**, 5432–5442 (1997).

[18] Th. Henning, B. Begemann, H. Mutschke, and J. Dorschner, Optical properties of oxide dust grains, Astron. Astrophys. Suppl. Ser. **112**, 143–161 (1995).

[19] G.A. Niklasson and C.G. Granqvist, Optical properties and solar selectivity of coevaporated Co–Al_2O_3 composite films, J. Appl. Phys. **55**, 3382–3410 (1984).

[20] U. Rossow, Depolarization/mixed polarization corrections of ellipsometry spectra, Thin Solid Films **313–314**, 97–101 (1998).

[21] I. Simkiene, J. Sabataityte, G.J. Babonas, A. Reza, and J. Beinoras, Self-organization of porphyrin structures on Si, Mater. Sci. Eng. C (submitted).

Fe/Fe-O NANODALELIŲ SAVAIMINIS SUSIDARYMAS PORĖTOSIOSE SiO₂ PLĖVELĖSE

I. Šimkienė [a,b], J. Sabataitytė [a,c], M. Baran [d], R. Szymczak [d], J.G. Babonas [a,c], A. Rėza [a,e], A. Kaliničenko [f]

[a] *Puslaidininkių fizikos institutas, Vilnius, Lietuva*
[b] *Vilniaus universitetas, Vilnius, Lietuva*
[c] *Vilniaus Gedimino technikos universitetas, Vilnius, Lietuva*
[d] *Lenkijos MA Fizikos institutas, Varšuva, Lenkija*
[e] *Vilniaus pedagoginis universitetas, Vilnius, Lietuva*
[f] *Chemijos institutas, Vilnius, Lietuva*

Santrauka

Išnagrinėtas Fe/Fe-O dalelių savaiminis susidarymas porėtosiose SiO₂ plėvelėse, tiriant hibridinių SiO₂:Fe/SiO₂/Si darinių sandarą ir fizikines savybes. Fe priemaišintos Si oksido plėvelės buvo suformuotos centrifūgoje ant SiO₂ sluoksniu padengtų Si plokštelių, panaudojant zolio–gelio metodiką. Zolis buvo paruoštas iš etanolo ir / arba vandeninių tetraetoksisilano ir FeCl₃ tirpalų. Suformuoti hibridiniai dariniai buvo atkaitinti Ar atmosferoje. San-daros tyrimai atominės jėgos mikroskopu parodė, kad bandinių su įvairiu Fe kiekiu morfologija yra skirtinga. Spektroskopinė elipso-metrija atlikta, siekiant apibūdinti Fe/Fe-O klasterių indėlį į hibri-dinių darinių optinį atsaką. Fe priemaišintų SiO₂ plėvelių magne-tinės savybės buvo tiriamos, matuojant magnetinio momento pri-klausomybes nuo magnetinio lauko ir temperatūros. Eksperimenti-niai rezultatai aiškinami, atsižvelgiant į Fe ir Fe oksidų nanodalelių ypatumus silicio oksido matricoje.